Poly(ionic liquid)s Derived from 3-Octyl-1-vinylimidazolium Bromide and N-Isopropylacrylamide with Tunable Properties

ARTICLE *in* JOURNAL OF POLYMER SCIENCE PART A POLYMER CHEMISTRY · OCTOBER 2014

Impact Factor: 3.11 · DOI: 10.1002/pola.27418

8 AUTHORS, INCLUDING:

Mariano Casu
Università degli studi di Cagliari
142 PUBLICATIONS **1,974** CITATIONS
SEE PROFILE

Mariano Andrea Scorciapino
Università degli studi di Cagliari
50 PUBLICATIONS **325** CITATIONS
SEE PROFILE

Roberta Sanna
Università degli Studi di Sassari
21 PUBLICATIONS **151** CITATIONS
SEE PROFILE

Alberto Mariani
Università degli Studi di Sassari
110 PUBLICATIONS **1,703** CITATIONS
SEE PROFILE

Poly(ionic liquid)s Derived from 3-Octyl-1-vinylimidazolium Bromide and *N*-Isopropylacrylamide with Tunable Properties

Javier Illescas,[1] Mariano Casu,[2] Valeria Alzari,[1] Daniele Nuvoli,[1] Mariano Andrea Scorciapino,[2] Roberta Sanna,[1] Vanna Sanna,[1] Alberto Mariani[1]

[1]Dipartimento di Chimica e Farmacia, Università di Sassari, and Local INSTM Unit, 07100 Sassari, Italy
[2]Dipartimento di Scienze Chimiche e Geologiche, Università di Cagliari, Cittadella Universitaria di Monserrato, 09042 Monserrato, Italy
Correspondence to: A. Mariani (E-mail: mariani@uniss.it)

Received 16 July 2014; accepted 13 September 2014; published online 3 October 2014
DOI: 10.1002/pola.27418

ABSTRACT: A new series of linear and crosslinked copolymers, obtained from 3-octyl-1-vinylimidazolium bromide (VImBr) and *N*-isopropylacrylamide (NIPAAm), were prepared by radical polymerization. Namely, VImBr was synthesized from 1-bromooctane and an ionic liquid such as 1-vinylimidazole. NIPAAm was used because it gives raise to well known thermoresponsive (co-)polymers. The copolymers were thoroughly characterized by means of ^{1}H NMR and ^{13}C NMR spectroscopies. Besides, differential scanning calorimetry, Fourier transform infrared spectroscopy, and scanning electron microscopy were also used. Moreover, the swelling behavior and the thermoresponsive properties of the corresponding hydrogels were studied. It was found that the VImBr incorporation into the copolymers does have a dramatic influence on both the thermal properties of the dried materials and the lower critical solution temperature of the corresponding hydrogels. In detail, the glass transition temperature was dependent on the monomer ratios, and ranged from 5 to 155 °C. Analogously, the lower critical solution temperature of the resulting hydrogels ranged from less than 10 up to 38 °C, thus including the physiological temperature. NMR spectroscopies, which were performed on the linear polymers, indicated that the monomers exhibit an alternating tendency resulting in a microstructure in which blocks are not present, at least when the two monomers are in equimolar amounts. © 2014 Wiley Periodicals, Inc. J. Polym. Sci., Part A: Polym. Chem. **2014**, *52*, 3521–3532

KEYWORDS: hydrogels; NMR; poly(ionic liquid)s; radical polymerization; vinyl imidazole

INTRODUCTION In recent years, ionic liquids (ILs) have attracted the attention of the scientific community due to their outstanding properties: excellent thermal stability, very good dissolution capability of many organic and inorganic compounds including cellulose and synthetic polymers, low flammability and volatility, and high ionic conductivity. Also, ILs are used as solvents for chemical synthesis, biocatalysis, homogeneous catalysis, separation technologies, nanomaterial preparations, templates for production of porous solids, hydraulic fluids, and lubricants.[1] Originally, ILs were exploited in green chemistry,[2,3] but later they have found an increasing number of applications in different fields as, for example, metal ion extractans,[4] electroactive and catalytic materials,[5–7] organic and polymer chemistry,[6,8] biotechnology,[9] nanomaterial technology,[10] initiators in polymerization process,[11] and as a medium for exfoliating materials.[12] In particular, in polymer science ILs have been investigated in different applications such as the development of novel functional polymers,[13–15] as green solvents in polymerization processes,[3] and as novel solvents for biopolymers.[16] Specifically, as polymerization has been one of the earliest research fields involving ILs, it is an area that has been thoroughly reviewed.[17,18] Indeed, since 1973, synthesis, characterization, and polymerization of IL monomers have been reported[18–20] to obtain a material that could be capable of combining the properties of ILs with improved mechanical stability and dimensional control resulting from the polymerization process. Some of the most important advantages of synthesizing a polymeric ionic liquid are the improved processability, the enhanced control over their structure, and their better stability.

Usually, poly(ionic liquid)s (PILs) are a special type of polyelectrolytes which carry an IL moiety in each of the repeating units. Common IL cations that have been studied include ammonium, phosphonium, pyridinium, pyrrolidinium, and imidazolium.

Additional Supporting Information may be found in the online version of this article.

Among them, the imidazole ring is a very flexible support for ILs in that it could be easily ionized, resulting in a permanent positive charge. Moreover, a simple arrangement of different alkyl substituents and counteranions enables tuning the properties of the IL. Imidazole has gained this attention for different reasons, especially its adjustable structure, thermal stability, relatively high ionic conductivity, and its amphoteric behavior in solution, that is the imidazole ring both accepts and donates protons. In addition, the imidazolium cation is associated with a mobile counteranion, which can be introduced to further tuning solubility and conductivity.[21] Imidazole-based ILs have found uses in several applications, including potential water treatment agents due to their ability to coordinate with metal atoms, and electromechanical device fabrication.[22–24] On the other side, anions, which generally influence the IL properties more than cations, can range from commonly used halides, mineral acid anions, and polyatomic inorganics (PF_6^- and BF_4^-).

PILs have encouraged much interest in different science fields, that is materials science and polymer chemistry. Ohno et al. have developed a series of imidazolium-based monomers and macromonomers to produce polymer electrolytes with high ionic conductances.[25–28] Additionally, Pojman et al. have used IL monomers in frontal polymerization and photopolymerization kinetics processes.[29–32] Meanwhile, Mecerreyes et al. have used different polymerization techniques to obtain different PILs for diverse applications.[33–37] Moreover, they have been used for their response to external stimuli.[38–41]

Conversely, poly(*N*-isopropylacrylamide) (pNIPAAm) is a well-known polymer that exhibits a thermoreversible phase transition at about 32 °C.[42] This transition is called lower critical solution temperature (LCST): below LCST, pNIPAAm is water-soluble and hydrophilic while, when heated above LCST, it becomes hydrophobic and precipitates out from solution. Thus, a hydrophobically modified pNIPAAm can show thermoresponsive water solubility and form heterogeneous microstructures, which are composed of hydrophilic microdomains of pNIPAAm, together with hydrophobic segments.[43] pNIPAAm has been used in several applications, mainly because of the sharpness of its LCST, which, in addition, is relatively close to the physiological temperature, and the easiness to vary its phase separation temperature by copolymerization,[44–46] addition of salts,[47–49] or surfactants[47,50,51] to the polymer solution. However, it is important to note that one of the most important applications of pNIPAAm is in the synthesis of hydrogels, which are water-swollen polymeric materials that maintain a distinct three-dimensional structure. In fact, hydrogels were the first biomaterials designed for use in the human body.[52–54] Traditional methods of crosslinked hydrogel synthesis were limited by the control of the hydrogel detailed structure, which may derive from possible side reactions, unreacted pendant groups, and entanglements. Moreover, other inadequacies of traditional hydrogels are poor mechanical properties and slow or delayed response times to external stimuli.[53]

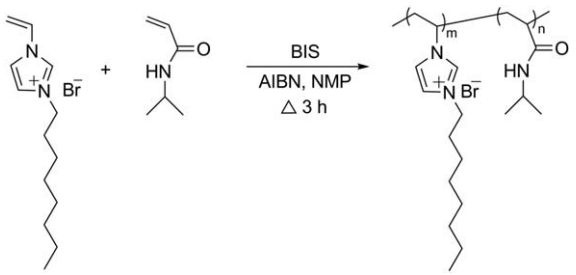

SCHEME 1 Copolymerization reaction between VImBr and NIPAAm monomers.

In our research group, we synthesized different kinds of stimuli-responsive hydrogels. Namely, those of poly(*N*,*N*-dimethylacrylamide),[55] poly(acrylamide-*co*-3-sulfopropyl acrylate),[56–59] poly(NIPAAm-*co*-3-sulfopropyl acrylate),[60] poly(NIPAAm-*co*-*N*-vinylcaprolactam),[61] poly(2-hydroxyethylacrylate-*co*-acrylic acid),[62,63] poly(*N*-vinylcaprolactam) reinforced with nanocrystalline nanocellulose,[64] and poly(2-acrylamido-2-methyl-1-propanesulfonic acid) containing graphene[65] were successfully obtained.

In this article, we report the synthesis and characterization of PIL-based polymer materials derived from the radical homo- and copolymerization of VImBr and NIPAAm (Scheme 1). Both linear and crosslinked materials were synthesized. The first were fully characterized by proton and carbon nuclear magnetic resonance spectroscopies (^{1}H NMR and ^{13}C NMR). The crosslinked materials were characterized both as dried materials and hydrogels. Namely, the swelling behavior, thermosensitive responses, and LCST of these latter were studied. Additionally, the dried materials were characterized by means of ^{1}H NMR, ^{13}C NMR; furthermore, the materials were studied by Fourier transform infrared spectroscopy (FTIR), differential scanning calorimetry (DSC), to determine their glass transition temperature (T_g) and conversion degree, and scanning electron microscopy (SEM) for morphological analysis.

It should be noticed that, during the preparation of this manuscript, a similar work dealing with the copolymerization of NIPAAm and 1-butyl-3-vinylimidazolium bromide (BVImBr) has been published, which has been used as comparison in several points of the following discussion.[66]

EXPERIMENTAL

Materials

N-Isopropylacrylamide (NIPAAm, ≥97%, FW = 113.16, mp = 60–63 °C), 1-vinylimidazole (VIm, FW = 94.11, d = 1.039 g/mL, bp = 192–194 °C), 1-bromooctane (1-BrOc, 99%, FW = 193.12, d = 1.118 g/mL, bp = 201 °C), *N*,*N*′-methylene bis-acrylamide (BIS, FW = 154.17, mp = 300 °C), azobisisobutyronitrile (AIBN, FW = 164.21, mp = 102–104 °C), and 1-methyl-2-pyrrolidinone (NMP, FW = 99.13, bp = 202 °C, d = 1.028 g/mL) were purchased from Sigma–Aldrich and used as received.

VImBr Monomer Synthesis

1-Vinyl-3-octylimidazolium bromide (VImBr) ionic liquid monomer derived from 1-vinylimidazole was synthesized according to the procedure reported in the literature:[67] in a typical reaction vessel, 1-BrOc (22 mmol) and VIm (20 mmol) were placed in a test tube, mixed thoroughly, and the mixture was heated intermittently in an unmodified household MW oven (Panasonic WS-650S-1150W) at 300 W (30 s irradiation with 10 s mixing) until a clear single phase was obtained. The recorded bulk temperature was in the range between 90 and 120 °C. The resulting viscous liquid was then cooled, washed with ethyl acetate (3 × 3 mL) and then with ether (3 × 3 mL) to remove both unreacted starting materials and solvent traces. Finally, the obtained VImBr was dried under vacuum at 80 °C for 48 h.

Homo- and Copolymer Synthesis

Crosslinked Materials

These samples were prepared using different molar fractions of NIPAAm and VImBr, from NIPAAm homopolymer (pNIPAAm) to VImBr homopolymer (pVImBr), keeping constant the amounts of crosslinker (BIS, 5 mol % referred to the total amount of NIPAAm and VImBr homopolymers), AIBN initiator (3.5 mol % referred to the total amount of monomers) and NMP (2 mL) as solvent medium.

A common glass test tube (i.d. = 1.5 cm, length = 16 cm) was filled with the appropriate amounts of (co-)monomers NIPAAm and/or VImBr, BIS and NMP. The mixture was sonicated with an ultrasound bath (EMMEGI, 0.55 kW, water temperature ≈ 25 °C) until the mixture became homogeneous. Then, AIBN was added and the mixture was sonicated again until a homogeneous phase was formed.

The polymerizations were performed in an oil bath for 3 h at 80 °C and for other 3 h at 110 °C. Once the polymerization was achieved, all samples were washed for 48 h with distilled water to remove NMP. Then, the samples were dried for 72 h in an oven under vacuum at 70 °C.

Linear Materials

These samples were synthesized using the same procedure described for the crosslinked materials but without the addition of the crosslinker.

Characterization

Hydrogels

The swelling behavior of the hydrogels was measured in water from 3 to 60 °C, using a thermostatic bath. Three different heat rates were used: 6 °C/day (from 3 to 28 °C), 2 °C/day (from 28 to 40 °C), and 10 °C/day (from 40 to 60 °C).

The weights of the swollen samples were measured at different time intervals after excess surface water was removed. The procedure was repeated until there was no further weight variation.

The SR% was calculated by applying the following equation:

$$\mathrm{SR\%} = \left[\frac{(W_s - W_d)}{W_d}\right] \times 100,$$

where W_d and W_s are the gel masses in the dry and in the swollen state, respectively.

Afterwards, lower critical solution temperature (LCST) was determined as the inflection of the curves obtained by interpolating SR% experimental data.

The morphological characterization of polymer hydrogels was performed using a scanning electron microscope SEM JEOL 7600. Before the analysis, samples were lyophilized, fractured in liquid nitrogen, and the fractured surface was coated with gold. The samples were also characterized using an Environmental SEM ZEISS EVO LS10 instrument.

Crosslinked Dried Samples

DSC thermal characterization was performed by means of a Q100 Waters TA Instruments calorimeter, using TA Universal Analysis 2000 software. Two heating ramps from −80 to 300 °C, using a heating rate of 20 °C/min, were performed on dry samples. The first scan was performed to remove traces of residual solvent and determine monomer conversion by calculating the residual polymerization heat. The second one was recorded to determine the glass transition temperature (T_g) of homo- and copolymers.

The FTIR spectra were recorded on a Bruker Vector-22 Fourier Transform Infrared Spectrometer, equipped with a diamond ATR device (Type A225/Q). The absorption was measured in a wavenumber range between 4000 and 600 cm^{-1} with a resolution of 4 cm^{-1}. To enhance the signal to noise ratio, each spectrum was acquired with 64 scans. Samples were pressed to bring them into contact with the diamond crystal of the ATR unit. Every sample was recorded twice to consider reproducibility.

Linear Dried Samples

High resolutions NMR spectra were acquired with a Unity Inova 500NB high-resolution spectrometer (Agilent technologies, Santa Clara, CA) operating at a ^1H frequency of 500 MHz, equipped with an upfield indirect detection probe. Experiments were performed at 40 °C. The chemical shift scale of either ^1H or ^{13}C was referenced to the methyl signal of DMSO. ^1H NMR spectra were acquired using a 6.7 μs pulse (90°), 1 s delay time, 2 s acquisition time, and a spectral width of 6.5 kHz. ^{13}C NMR spectra were acquired using a 5.6 μs pulse (45°), 3 s delay time, 2 s acquisition time, and a spectral width of 29 kHz.

$^1H-^1H$ NMR correlation spectroscopy (COSY) experiments were recorded over the same spectral window using 2048 complex points, 3 s delay time and sampling each of the 512 increments. The same acquisition parameters have been applied, together with a mixing time of 80 ms (MLEV-17 spin-lock scheme), for the acquisition of total correlation spectroscopy (TOCSY). The $^1H-^{13}C$ NMR correlation heteronuclear single quantum coherence (HSQC) spectra were

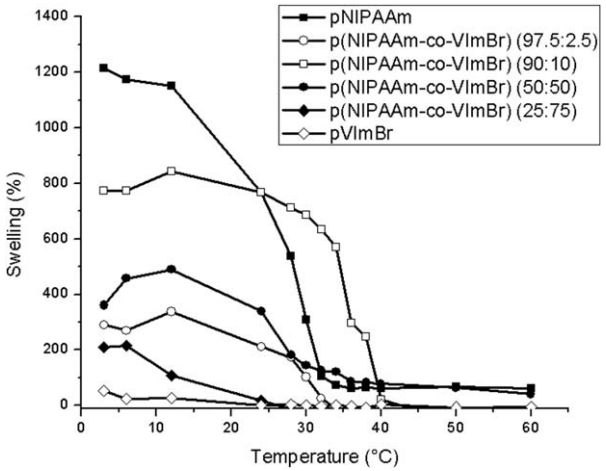

FIGURE 1 Swelling behavior and determination of the LCST for the homo- and copolymers of NIPAAm and VImBr with different molar ratios.

collected using 3 s delay time and a spectral window of 6.5 and 29 kHz for ^{1}H and ^{13}C, respectively, and sampling each of the 512 increments.

The overlapping bands observed in the region 48–52 ppm were decomposed using the Origin 7 (Microcal) software package. Gaussian functions were used throughout with the minimum number of component bands used for the fitting process. Other functions were also examined but the results were inferior. Line widths, intensities, and frequencies were allowed to vary in the iteration process until reproducible results were obtained with squared correlations (r^2) greater than 0.999.

RESULTS AND DISCUSSION

The main object of this work was the synthesis and characterization of crosslinked polymer materials made from VImBr and/or NIPAAm. However, some of the corresponding linear polymers were also prepared to be studied by NMR spectroscopies in solution. If not indicated, we refer to the crosslinked polymer materials. When the discussion will be about the linear ones, it will be properly indicated.

First of all, VImBr monomer was synthesized according to the literature[67] (NMR in Supporting Information Fig. S1) and used as the comonomer of NIPAAm in the copolymer synthesis.

Initially, the time necessary for the hydrogels to get the swelling equilibrium in water at 22 °C was determined. It was found that the maximum SR% is reached after about 24 h.

Apart from the p(NIPAAm-*co*-VImBr) with 90 mol % NIPAAm, which exhibits the highest SR%, the swelling ratio of all the other polymers is roughly proportional to the NIPAAM:VImBr ratio; namely, it is higher in the materials containing the larger amounts of NIPAAm. In other words, the addition of VImBr results in an initial increase of the swelling ratio and in its subsequent decrease. This behavior can be attributed to the double nature of VImBr, which is made of an ionic moiety (the cationic imidazolium ring) linked to a hydrophobic one (the octyl chain): the first is responsible for the increase of SR% at lower content, and the second for its decrease due to the larger hydrophobic character.

Figure 1 shows the swelling percentage of hydrogels as a function of temperature. It can be observed that there is a remarkable decrease of swelling as temperature augments. In particular, NIPAAm homopolymer exhibits an LCST around 30 °C, which is in agreement with the value previously reported in the literature.[42]

The LCST is clearly visible in all the NIPAAm-containing samples. However, it is very sharp in the aforementioned p(NIPAAm-*co*-VImBr) with 90 mol % NIPAAm, while is less evident and occurs in a larger temperature range in all the other hydrogels. Moreover, the p(NIPAAm-*co*-VImBr) (90:10) hydrogels exhibit a significant shift of the LCST value, which reaches about 38 °C.

It is noteworthy that an analogous result was recently published by Seo et al.[66] in the case of the NIPAAm–BVImBr copolymer. Indeed, also in that case the monomer ratio giving rise to the largest and sharpest LCST was 90:10. This could be ascribed to the optimal balance among hydrophilic and hydrophobic forces due to the addition of VImBr to the NIPAAm, thus imparting it new, interesting features.[68] In particular, the repulsion between the cationic units could be considered to increase LCST.[66] Moreover, as far as the extent of temperature range at which the LCST occurs, it is known that it strongly dependent on the copolymer microstructure and molar comonomer ratio, which in the present case differ from (co-)polymer to (co-)polymer.[68–74]

At variance, p(NIPAAm-*co*-VImBr) (25:75) is characterized by a shift of the critical solution temperature to lower values (<10 °C). These findings suggest that the effect of the molar composition on the thermoresponsive behavior of the obtained hydrogels is particularly evident and can be tuned by varying the ratio between the monomers. It should be underlined that this is an uncommon case in which the presence of a second monomer influences the LCST of a NIPAAm-based polymer hydrogel in two opposite directions, that is, by lowering and by increasing it, as the monomer ratio varies in a proper way. Generally speaking, the possibility to tune the phase separation by the molecular architecture is an attractive challenge for advanced applications of polymer materials. In this case, it is also noteworthy that the LCST value of 38 °C comprises the physiological temperature, a characteristic that is not typical of NIPAAm homopolymer and that might be of potential interest in biomedical field.

All dried samples were characterized by means of DSC. In particular, it was found that conversions were always almost quantitative, and T_g values were dependent on the VImBr content in the copolymer (Fig. 2). As it can be seen, only one

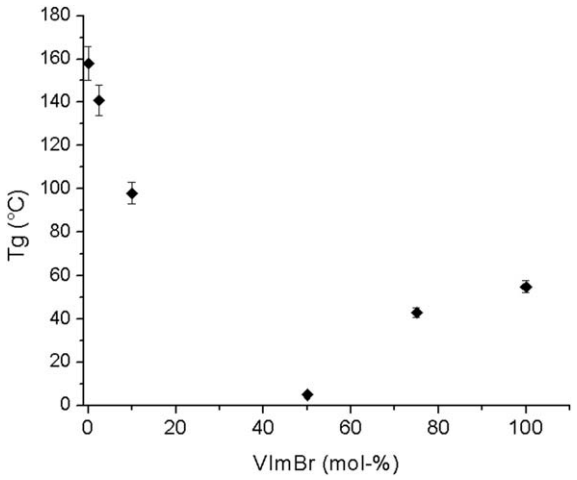

FIGURE 2 T_g as a function of the VImBr amount.

T_g value is exhibited by each sample, thus suggesting that VImBr and NIPAAm did not give rise to block copolymers but, more probably, to random or roughly alternate microstructures. Additionally, T_g values tend to decrease as the VImBr content increases, reaching the lowest value when the molar ratio is 50:50. For example, while the T_g value of pNIPAAm was 155 °C, that of the p(NIPAAm-*co*-VImBr) (50:50) was 5 °C only. This is probably due to the plasticizing effect that the VImBr long octyl chain exerts in the copolymer structures.[75] However, for VImBr contents that are higher than 50 mol %, T_g tends to increase again, up to 55 °C, which is the value found for the VImBr homopolymer. A possible explanation for this behavior can be the increased interactions among macromolecular chains due to the larger presence of ionic sites due to the VImBr units. It should be highlighted that this range includes the room temperature, thus indicating that, by properly choosing the monomer ratio, a glass or a rubber polymer material can be obtained.

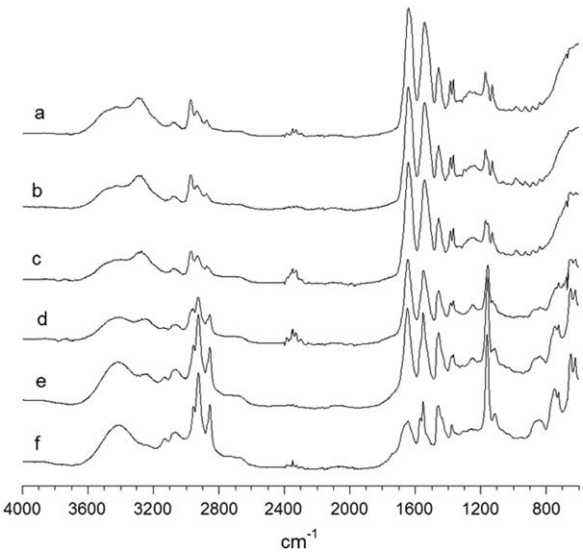

FIGURE 3 FTIR spectra of the synthesized homo- and copolymers with different molar compositions: (a) pNIPAAm, (b) p(NIPAAm-*co*-VImBr) (97.5:2.5), (c) p(NIPAAm-*co*-VImBr) (90:10), (d) p(NIPAAm-*co*-VImBr) (50:50), (e) p(NIPAAm-*co*-VImBr) (25:75), and (f) pVImBr.

It should be highlighted that this behavior is qualitatively in agreement with that of SR%, in which the balance between hydrophilic and hydrophobic characteristics plays a decisive role on the material properties.

Figure 3 shows the FTIR spectra of pNIPAAm, pVImBr, and the copolymers with different monomer molar ratios. NIPAAm homopolymer shows its characteristic stretching absorption band at 1640 cm^{-1} attributed to amide I band (vibration mode which consists mainly of the C═O stretching), at 1542 cm^{-1} attributed to amide II (mostly N—H in plane deformation), at 1459 cm^{-1} attributed to the coupled band of C—H and CH_3, 1366–1386 cm^{-1} attributed to the CH_3 bending mode.[76]

pVImBr is characterized by the presence of vibration bands at 1378, 1301, and 1160 cm^{-1}, respectively.[77] In the case of the p(NIPAAm-*co*-VImBr) (50:50) copolymer, this shows: (i) one stretching absorption band of the amide I shifted to 1645 cm^{-1}, while the amide II band is shifted to 1538 cm^{-1}, (ii) the absence and shift of the band at 1164 cm^{-1} when the VImBr molar fraction diminishes, and it is not present in the pNIPAAm gel.

Also, the presence of a band at 2855 cm^{-1} in the copolymer spectra, which is not present in the NIPAAm homopolymer spectrum (due to the presence of the methylene groups of the octyl chain), confirms the successful copolymerization occurrence.

The FTIR spectrum of pNIPAAm in the range 3100−3600 cm^{-1} shows a very broad band at 3450 cm^{-1} and a broad band at 3289 cm^{-1}. This latter is characteristic of N—H vibration, while the very broad band which appears at ~3400 cm^{-1} is characteristic of O—H vibration of water molecules. This latter band is also characteristic of the FTIR spectra of pVImBr.[76] In the cases of p(NIPAAm-*co*-VImBr)'s, the band at 3289 cm^{-1} shifts to lower frequency (3256 cm^{-1}) in the 50:50 copolymer, suggesting the involvement of the NH group in a weak hydrogen bond as confirmed also by the amide II shift.[78]

The morphological structures of NIPAAm and VImBr homopolymers and their copolymers with different molar proportions were investigated by SEM. Figure 4(a) shows the micrograph of pNIPAAm. From this image, it can be seen that this homopolymer shows its typical network structure characterized by the presence of well-defined pores. In contrast, Figure 4(b,c) depicts a cross-sectional SEM micrographs of pVImBr and the p(NIPAAm-*co*-VImBr) with a 90:10 molar ratio. They have a less defined structure, characterized by the presence of some irregular pores. Therefore, it can be concluded that VImBr does influence hydrogel structures, at least at this level. However, by taking into account the swelling behavior discussed above, no relation seems to exist between SR% and pore structure, thus confirming what we already observed in our previous work.[79]

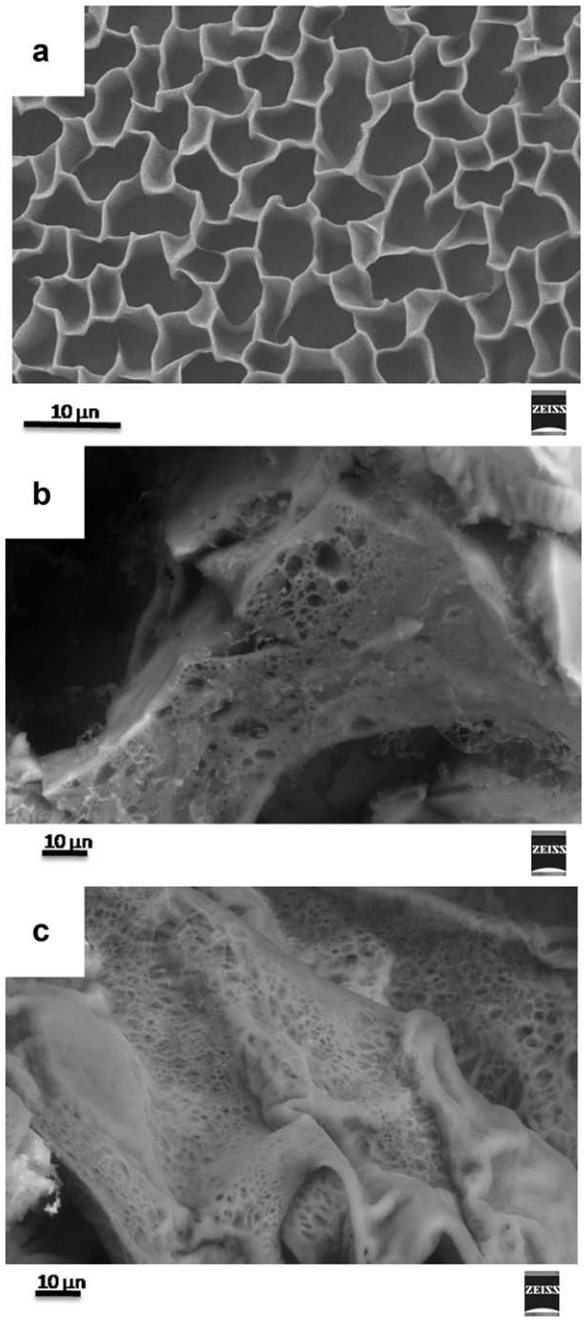

FIGURE 4 SEM micrographs of: (a) NIPAAm homopolymer, (b) VImBr homopolymer, and (c) p(NIPAAm-*co*-VImBr) (90:10). Scale bars are 10 μm.

To have a better polymer characterization, the ^{1}H and ^{13}C NMR spectroscopies in liquid phase were exploited. To do this, non-crosslinked, linear homo- and copolymers having the same monomer composition of the crosslinked ones were prepared. The following discussion refers to these samples. The ^{1}H and ^{13}C NMR spectra of NIPAAm monomer and pNIPAAm are shown in Figures 5 and 6, and the corresponding data are reported in Table 1.

The resonances of the olefin protons, in the range between 5 and 7 ppm, are very clear in the monomer and totally disappear in the polymer. In this latter spectrum, the new broad signals at 1.98 ppm are assigned to the CH(c), and the two broad signals between 1.2 and 1.7 ppm are assigned to the CH(d) protons of the polymer backbone (Fig. 5). These results are in good agreement with what already reported in the literature[80] and confirm the homopolymerization of NIPAAm. The signals at 3.83 ppm and 1.09 ppm in the homopolymer are attributed to the CH(b) and the two methyl groups, respectively. The NH signal resonates at 7.81 ppm in the NIPAAm monomer and between 6.6 and 7.8 ppm in the pNIPAAm.

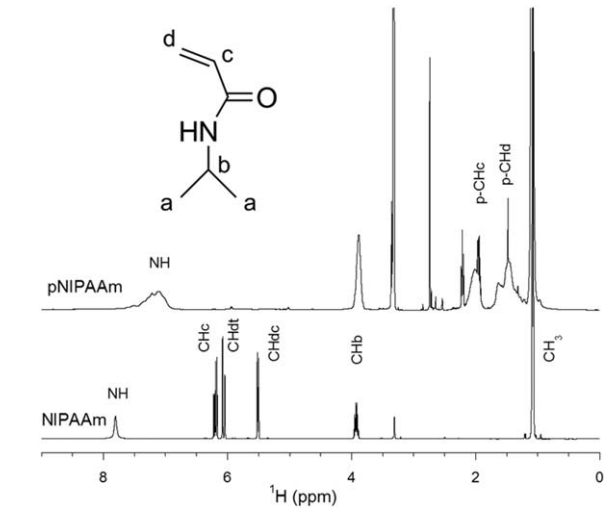

FIGURE 5 ^{1}H NMR of NIPAAm monomer and linear pNIPAAm.

In the case of the ^{13}C NMR characterization, it can be inferred that the resonances of the olefin carbon in the monomer are in the region between 124 and 133 ppm, but disappear in the polymer spectrum (Fig. 6).

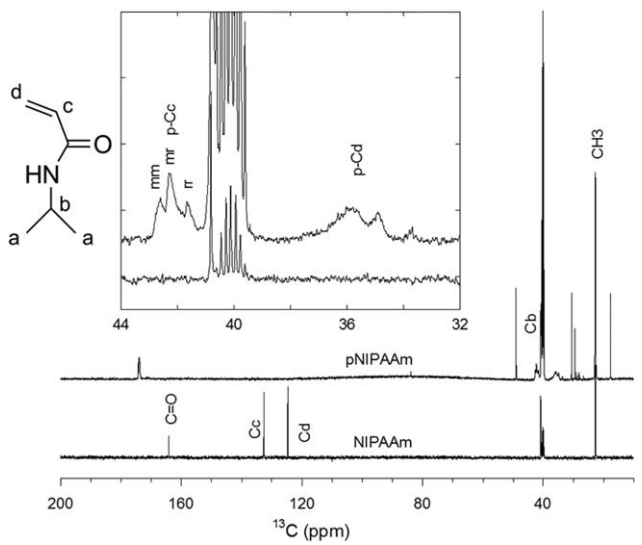

FIGURE 6 ^{13}C NMR of NIPAAm monomer and linear pNIPAAm.

TABLE 1 ^{1}H and ^{13}C NMR: NIPAAm Monomer and Linear pNIPAAm Data

	NIPAAm		pNIPAAm	
Bond	^{1}H (ppm)	^{13}C (ppm)	^{1}H (ppm)	^{13}C (ppm)
N—CH_3	1.08	22.68	1.09	22.70
N—CH_b	3.95	40.81	3.83	40.78
N—CH_c	6.20	132.66	1.98	41–43
N—CH(dtrans)	6.06	124.70	1.2–1.7	33–37
N—CH(dcis)	5.51	124.70	1.2–1.7	33–37
NH	7.81	–	6.6–7.8	–
N—C=O	–	163.95	–	173.3

In Figure 6, the signal of the C(c) in the homopolymer, attributed by the HSQC spectrum, was found in the range between 41 and 43 ppm, and the C(d) signals at about 33 and 37 ppm. Both carbon groups show stereochemical sensitivity, the C(c) carbon resonances have been attributed by Hirano et al.[81] to the syndiotactic triad rr = 42.63 ppm, the heterotactic triad rm = 42.3 ppm, and the isotactic triad mm = 41.6 ppm.

In addition, in Figure 6, it is observed that the aliphatic C(b) carbon signals are peaked at 40.81 ppm in the monomer and at 40.78 ppm in the homopolymer. Additionally, the CH_3 carbon signal has been found at 22.68 ppm and 22.70 ppm, respectively.

The obtainment of VImBr homopolymer was confirmed by ^{1}H and ^{13}C NMR analysis and their data are reported in Table 2. The spectra of these results are shown in Figures 7 and 8.

TABLE 2 ^{1}H and ^{13}C NMR: VImBr Monomer and Linear pVImBr Data

	VImBr		pVImBr	
Bond	^{1}H (ppm)	^{13}C (ppm)	^{1}H (ppm)	^{13}C (ppm)
a	0.91	14.84	0.91	14.60
b	1.32	22.80	1.26	22.52
c	1.36	26.40	1.31	26.29
d	1.33	29.23	1.29	28.98
e	1.30	29.38	1.24	31.88
f	1.32	29.91	1.31	32.11
g	1.92	29.16	1.84	29.43
h	4.29	49.72	4.18	50.48
i	8.05	124.21	7.7 broad	123
l	8.33	120.10	7.9 broad	120
m	9.77	136.22	9.73	136
n	7.40	130.41	4.81, 4.66, 4.48	52.8–55.8
o (*trans*)	6.06	109.56	2.3–3.2	38–40
o (*cis*)	5.48	109.56	2.3–3.2	38–40

The comparative analysis of ^{1}H NMR spectra of VImBr monomer and homopolymer indicates some significant changes in the chemical shifts of the imidazole ring and the olefinic protons signals around 5.2 and 7.7 ppm. The signals at 0.91, 1.30–1.32, 1.92, and 4.29 ppm are attributed to the aliphatic chain of the VImBr, as labeled in the spectrum (Fig. 7 and Table 2). It can be noted that the resonances of the olefinic protons in the monomer disappear in the polymer, and that the new broad signals in the range between 2.3 and 3.2 ppm are attributed to the CH(o) group of the macromolecular backbone and the splitted signals (mm = 4.81 ppm, mr = 4.66 ppm, and rr = 4.49 ppm triads) are attributed to the CH(n) of this chain.[82]

The assignment of the ^{13}C NMR signals of VImBr monomer, attributed by the HSQC sequence (Supporting Information Fig. S2), is shown in Figure 8. The aliphatic carbons C(a)—C(g) of the VImBr monomer resonate in the region between 14 and 30 ppm; nevertheless, the C(h) signal is at 49.72 ppm. This latter, which is broader in the VImBr homopolymer spectrum, moves to 50.48 ppm. The other signals of the aliphatic chain are broadened and show small shifts, as it is reported in Table 2. The ^{13}C NMR signals of the imidazole ring in the monomer are found at 124.21 ppm for the C(i), 120.10 ppm for the C(l), and at 136.22 ppm for the C(m). In the case of the VImBr homopolymer, these signals are very broad and resonate at 123 ppm, 120 ppm, and 136 ppm, respectively. In addition, the signals of the olefin carbons in the monomer are at 130.41 ppm for the C(n) and 109.56 ppm for the C(o), respectively. In the VImBr homopolymer, the signal of C(n) resonates in the range between 52.5 and 55.8 ppm, while the C(o) between 38 and 40 ppm, overlapped with the signal of DMSO, attributed by HSQC sequence.

The ^{1}H NMR spectra of the linear p(NIPAAm-*co*-VImBr) with different molar compositions are shown in Figure 9. As expected, the ^{1}H NMR spectrum of the copolymer sample with largest NIPAAm amount (90:10) looks very similar to that of the NIPAAm homopolymer. The main difference is the appearance of a new signal at 3.67 ppm, besides the one at 3.83 ppm, attributed to CH(b) of the aliphatic chain in the NIPAAM homopolymer. The signal at 3.67 ppm cross peaks with the CH_3 signals in the COSY map and is attributed to the CH(b) of the aliphatic chain of the NIPAAm unit (Supporting Information Fig. S3). The shift is attributed to compositional dependence of the CH(b) group of NIPAAm in the copolymer (90:10); indeed, the VImBr units result to be comprised between NIPAAm segments, thus giving rise to the shift of its signal, thus confirming that the copolymer microstructure is not characterized by the presence of VImBr blocks. The COSY map shows a cross peak between the signal at 4.31 and that at 1.87 ppm, which are attributed to CH(h) and CH(g) of the VImBr unit.

Conversely, the spectrum of the p(NIPAAm-*co*-VImBr) (25:75) shows features that are similar to that of the VImBr homopolymer, with several differences due to the presence

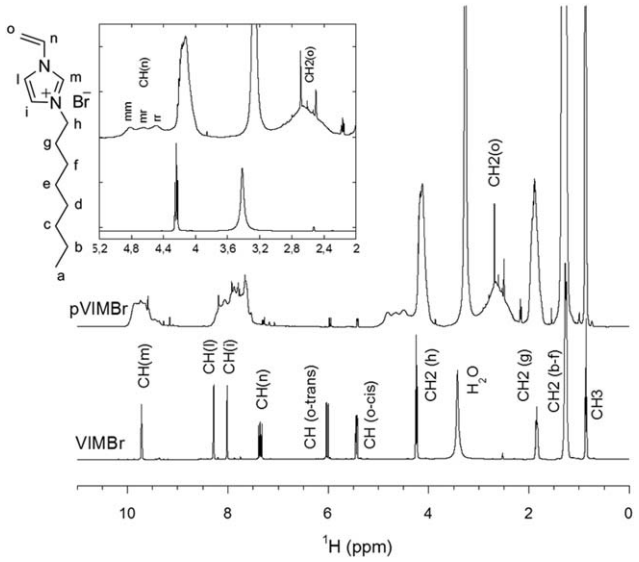

FIGURE 7 ^{1}H NMR of VImBr monomer and linear pVImBr.

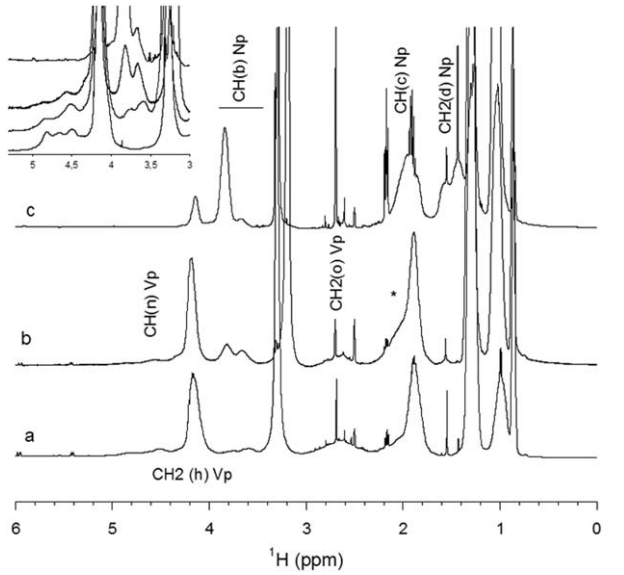

FIGURE 9 ^{1}H NMR of (NIPAAm:VImBr) copolymers with different molar compositions. (a) p(NIPAAm-*co*-VImBr) (90:10), (b) p(NIPAAm-*co*-VImBr) (50:50), and (c) p(NIPAAm-*co*-VImBr) (25:75). * pNIPAAm CH_2(d) e CH(c); pVImBr CH_2(n).

of the NIPAAm. For example, the CH(b) signal of the NIPAAm aliphatic group at 3.86 ppm is not present. In place of it, two new signals appear at 3.77 and 3.59 ppm which both cross peak with the CH_3 of the NIPAAm at 1.09 ppm. The signals are attributed to the CH(b) and indicate the complete incorporation of NIPAAm between the VImBr segments. Moreover, the signals at 1.59 ppm and 1.44 ppm, assigned to the CH(d) protons of the NIPAAm homopolymer backbone, are not present; this is a clear indication of the absence of NIPAAm blocks. This finding, together with the already discussed lack of VImBr blocks, confirms that random or roughly alternate copolymers have been prepared.

A broad shoulder in the range between 1.9 and 2.3 ppm that cross peaks in the TOCSY map with the broad signals in the range between 4.32 and 3.90 ppm of the CH(n) group of the VImBr unit is also present (Supporting Information Fig. S4). In addition, the signals of these CH(n) backbone groups are present at 4.83, 4.52, and 4.31 ppm.

This would suggest that the signal between 1.9 and 2.3 ppm may be attributed to the CH(o) of the VImBr backbone units. In the same range, also the CH(c) and CH(d) of the NIPAAm backbone units are present.

In the case of p(NIPAAm-*co*-VImBr) (50:50), the proton spectrum shows several differences when it is compared with the previous copolymers having different compositions. For instance, the broad proton signals comprised between 2.5 and 2.9 ppm, attributed to the CH(o) backbone group, are still present as well as the signals at 4.83 and 4.52 ppm, and a broad signal, overlapped with the CH(d) of the NIPAAm, in the range between 4.4 and 3.9 ppm, attributed to the CH(n) backbone group of the VImBr homopolymer. Besides, the signal that appears among 4.4 and 3.9 ppm shows a cross peak with the signals at 2.1 and 1.8 ppm in the COSY map, attributed to the CH(o) of the VImBr. These last signals are more intense with respect to that observed in the p(NIPAAm-*co*-VImBr) (25:75) sample. As far as the broad signal among 2.5 and 2.9 ppm (which cross peaks with the signals at 4.83 and 4.52 ppm) is concerned, this suggests the presence of some VImBr blocks as a consequence of the high VImBr content. In addition, the CH(b) signal of the aliphatic group of NIPAAm, which is found at 3.86 ppm, is still missing. In place of it, two new signals appear at 3.66 and 3.81 ppm, respectively, which cross peak with the CH_3 groups in the COSY map. Finally, the signals between 1.16 and 1.71 ppm, attributed to the backbone CH(d) of the pNIPAAm, are still missing.

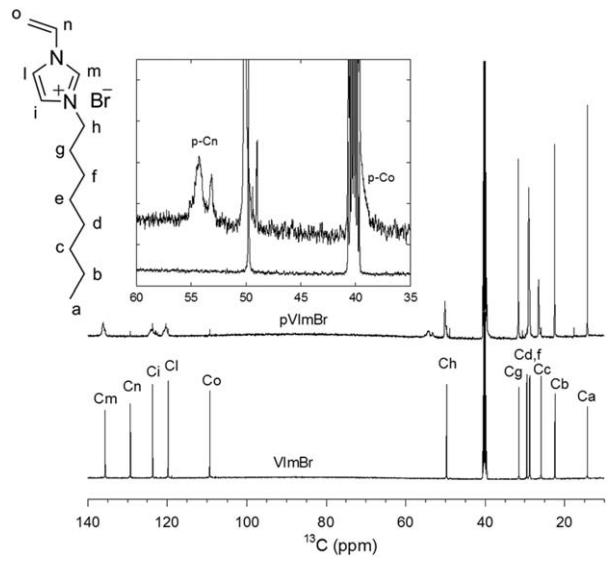

FIGURE 8 ^{13}C NMR of VImBr monomer and linear pVImBr.

As a general remark, it can be highlighted that NIPAAm and VImBr copolymers are characterized by a strong alternating tendency. However, while VImBr gives rise to some blocks, this is not the case for NIPAAm, thus suggesting that the former is characterized by higher reactivity ratios. This finding is in agreement with what already reported in literature for an analogous copolymerizing system.[83]

In the p(NIPAAm-*co*-VImBr) (50:50) sample, the signal of the NH group is shifted to 7.5−8.3 ppm overlapped with the signals of C(i) and C(l) of the imidazolium ring, while the same signal is at 6.6 and 7.8 ppm in the pNIPAAm. This suggests the involvement of the NH group in a weak hydrogen bond, as confirmed also by the FTIR spectra analysis.

The ^{13}C NMR spectra of the copolymers are shown in Figure 10. The main differences observed in the p(NIPAAm-*co*-VImBr) (90:10) spectrum respect to that of the NIPAAm homopolymer are the presence of a new signal at 49.58 ppm and the broad signals comprised between 57 and 60 ppm (Fig. 10).

The signal at 49.58 ppm is attributed, by the HSQC map (Supporting Information Fig. S5), to the VImBr carbon C(h); the spectrum is better pointed out in Figure 11. The broad signals around 57 and 60 ppm, pointed out in Figure 10, are attributed to C(n) carbon of VImBr. The C(c) of NIPAAm result shifted to upfields and it is partially overlapped with the DMSO signal, the C(d) signal is spread in the range comprised among 33.1 and 38.5 ppm.

The ^{13}C NMR spectrum of the p(NIPAAm-*co*-VImBr) (25:75) shows few differences with respect to that of the VImBr homopolymer. The most evident are the signal at 50.02 ppm, attributed to the C(h) of the VImBr, and the appearance of the signals between 51 and 59 ppm in the copolymer, which is attributed to C(n) carbons. In particular, these latter signals are larger than that observed in the homopolymer. The C(c) and C(d) signals of NIPAAm result overlapped with that of DMSO. The ^{13}C NMR spectrum of the copolymer p(NIPAAm-*co*-VImBr) (50:50) exhibits features similar to the other compositions: the signals appear broad and generally show differences in the shape and the chemical shift of the backbones of VImBr and NIPAAm.

In general, it is observed that most of the carbon signals are dependent on the comonomer composition. For example: (i) the signal at 50.02 ppm, which is attributed to the C(h) of the VImBr homopolymer, appears between: (a) 50.2 and 49.6 ppm in the p(NIPAAm-*co*-VImBr) (25:75), (b) 50.2 and 49.5 ppm in the p(NIPAAm-*co*-VImBr) (50:50), and (c) 49.8 and 49.4 ppm in the p(NIPAAm-*co*-VImBr) (90:10); (ii) the signals comprised between 52.8 and 56.0 ppm, attributed to the C(n) of the VImBr homopolymer, appear among: (a) 52.8 and 58.42 ppm in the p(NIPAAm-*co*-VImBr) (25:75), (b) 53.94 and 58.93 ppm in the p(NIPAAm-*co*-VImBr) (50:50), and (c) 57.3 and 59.56 ppm in the p(NIPAAm-*co*-VImBr) (90:10); (iii) the signal attributed to the C(o) of the VImBr homopolymer is found to be partially overlapped with the signal of DMSO. From the HSQC maps, it has been found that this signal is shifted to downfields when the NIPAAm amount increases in the copolymers; (iv) the signals of the C(c) group in the NIPAAm homopolymer are found in the range between 41 and 43 ppm. A shift of these signals towards upfields is observed when the VImBr amount increases; however, it is partially overlapped with the signal of DMSO; lastly, (v) the signal of the C(d) group in the NIPAAm homopolymer, comprised between 37.1 and 34.1 ppm, is shifted towards downfields. As previously observed, this signal is partially overlapped with the signal of DMSO, which has the same behavior found in the copolymer signals when the VImBr amount increases.

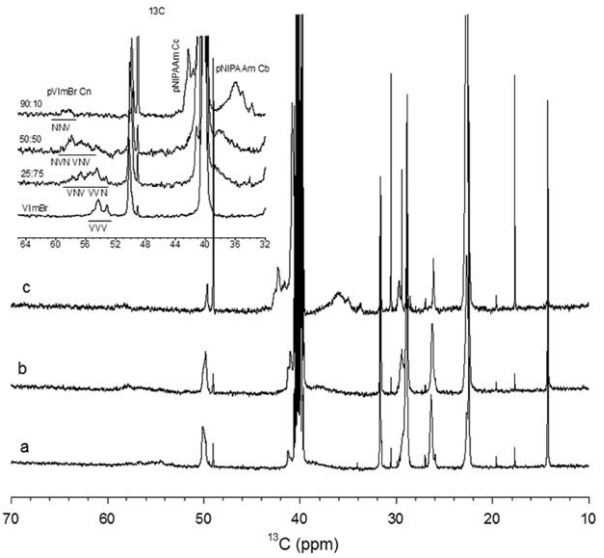

FIGURE 10 ^{13}C NMR of (NIPAAm:VImBr) copolymers with different molar compositions. (a) p(NIPAAm-*co*-VImBr) (90:10), (b) p(NIPAAm-*co*-VImBr) (50:50), and (c) p(NIPAAm-*co*-VImBr) (25:75).

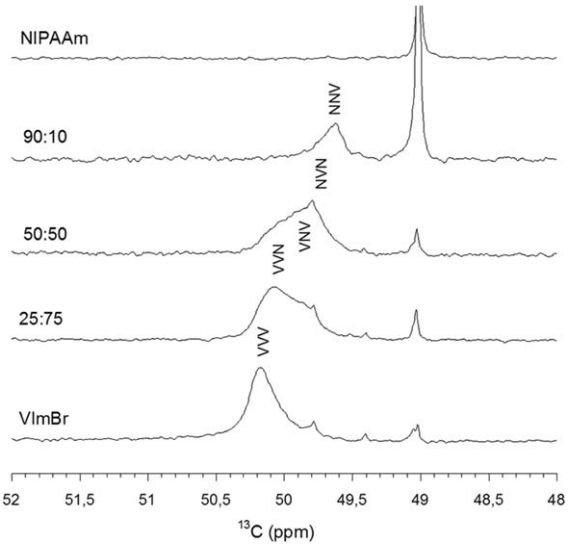

FIGURE 11 Expanded ^{13}C NMR of (NIPAAm:VImBr) copolymers with different molar compositions.

Furthermore, as it can be inferred from the ^{13}C NMR spectra, the signals of the VImBr and NIPAAm backbone units into the copolymer are dependent on the compositional sequence as well as the C(h) signal of VImBr. These results allow for a quantitation of the triads of the copolymers with different molar compositions. However, the only signal dependent on the composition that allows this analysis under the current experiments, due to the very broad signals owing to the presence of different types of monomer sequences, is the C(h) signal of VImBr.

The expanded region of the ^{13}C NMR spectra of the C(h) carbon in the VImBr with different mole fractions of VImBr (V) and NIPAAm (N) and the corresponding homopolymers is shown in Figure 11. The C(h) signals resonating at 50.16 ppm shift to upfields and exhibit complex pattern of overlapped signals, which can be ascribed to composition sensitivity of the C(h) group, with increase in the N content in the copolymer. The complex overlapping can be resolved by the application of band component analysis. The ^{13}C signals of the p(NIPAAm-*co*-VImBr) (90:10), p(NIPAAm-*co*-VImBr) (50:50), and p(NIPAAm-*co*-VImBr) (25:75) were fitted with three overlapping bands (Supporting Information Fig. S6). The overlapped band components in the p(NIPAAm-*co*-VImBr) (25:75) were found at 50.17, 50.06, and 49.81 ppm and are assigned to VVV (8%), VVN (69%), and NVN (23%) triads, respectively. Similarly, the overlapped band components in the p(NIPAAm-*co*-VImBr) (50:50) were found at 50.07, 49.83, and 49.62 ppm and assigned to VVN (32%), NVN (60%), and NNV (7%), respectively. The overlapped band components in the p(NIPAAm-*co*-VImBr) (90:10) were fitted with two bands at 49.83 and 49.62 ppm and might be assigned to NVN and NNV triads, respectively.

Finally, Figure 12 shows the ^{1}H NMR signal intensity as a function of temperature. In all cases, the integrated area of the strongest resonance, that is, the methyl protons of the NIPAAm units, is evaluated. The spectra are normalized to compensate the differences in the acquisition conditions. Thus, the signal level is proportional to the NIPAAm unit amount. As can be seen, a sharp intensity decrease was found as temperature rose, thus confirming the LCST occurrence already discussed in the case of crosslinked materials. In this case, the phenomenon can be observed because of the precipitation of the polymer and its consequent removal from the solution, which results in a corresponding decrease of the NMR signal. Moreover, the already observed dependence of the LCST value on the (co)polymer composition is also confirmed by these data.

For example, the ^{1}H NMR signal of NIPAAm homopolymer sample exhibits a markedly decrease at around 30 °C, which is a value that is close to that reported in the literature.[42,79,84,85] The same tendency was also observed for the p(NIPAAm-*co*-VImBr) (97.5:2.5), which reveals that the introduction of VImBr does not influence the LCST, at least at this low amount.

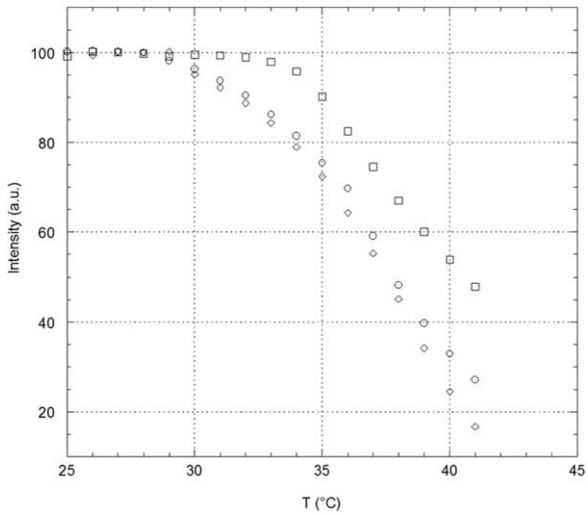

FIGURE 12 ^{1}H NMR signals (integral of the methyl proton resonance) of NIPAAm homopolymer (~1.2 ppm) and (NIPAAm:-VImBr) copolymers as a function of the temperature in D_2O. NIPAAm homopolymer (○), p(NIPAAm-*co*-VImBr) (97.5:2.5) (◇), and p(NIPAAm-*co*-VImBr) (90:10) (□). Heating rate was 1 °C every 30 min.

Finally, it is also observed that at a given p(NIPAAm-*co*-VImBr) molar composition (90:10), the methyl signal of NIPAAm shows a marked decrease at about 33 °C. In addition to the methylene group content, the location of the group within the monomer structure influences the LCST behavior of the copolymer.

CONCLUSIONS

Herein, we have reported the synthesis of different homopolymers and copolymers of NIPAAm and VImBr by the radical polymerization process. Both linear and crosslinked materials were prepared. These latter were characterized in terms of swelling behavior in water in the form of hydrogels and as dried samples using FTIR, SEM, and DSC analyses. Furthermore, an extensive use of NMR spectroscopy was done on the corresponding non crosslinked, linear samples. The effective copolymerization of VImBr with NIPAAm was confirmed by NMR, FTIR analyses, and by the peculiar characteristics in term of swelling behavior and T_g.

It was found that both the swelling behavior and the glass transition depend on the monomer ratio. Namely, at relatively low VImBr content, the ionic nature of the imidazolium moiety contributes to increasing the hydrophilic character of the NIPAAm-containing copolymer material, which results in a larger SR%. However, when the amount of VImBr is larger, its hydrophobic character, due to the long octyl chain, prevails, thus resulting in a subsequent decrease of the amount of swelling. As far as the glass transition temperature is concerned, the presence of the flexible octyl chain in the VImBr unit initially results in a plasticizing effect of the copolymer but, at largest content, probably because of the increased ionic interactions among

macromolecular chains due to the presence of ionic ring, it gives rise to an increase of glass transition temperature up to that of the VImBr value.

Moreover, LCST values of hydrogels undergo a significant change, which was demonstrated to be dependent on the VImBr content into the hydrogel structure. Namely, the critical solution temperature goes from less than 10 °C up to about 38 °C. As, the typical polyNIPAAm LCST is located at 30–32 °C, it is evident that the addition of the second monomer allowed us to tune this value, which can now be ranged from values that are lower to values that are higher than that of the homopolymer. Moreover, it is worthy to note that the new range includes now also the physiological one, which is generally not interested by the transition. Moreover, from morphological studies, performed by means of SEM, it has been demonstrated that the insertion of VImBr in the copolymers does have an effect into the hydrogel structure. Namely, hydrogel micrographs demonstrate a more regular network structure as VImBr content decreases.

It should also be underlined that VImBr exerts a dramatic effect on the glass transition temperature. Apart from what mentioned above in qualitative terms, it has been observed that by adding a proper amount of this second monomer, T_g values can be allowed to range from 155 to 5 °C. These values are higher and lower of the room temperature, thus indicating that the resulting copolymer maybe in the glass or in the rubber state, as the VImBr varies.

As far as the spectroscopic analysis is concerned, FTIR spectra of the copolymers exhibit a significant change with respect to those of NIPAAm and VImBr homopolymers. Mainly, the shift change in the N—H bands suggests the involvement of the amido group in a weak hydrogen bond.

Finally, from ^{1}H and ^{13}C NMR characterization it has been demonstrated that the copolymers signals change between monomers and homopolymers. Furthermore, the incorporation of the IL into NIPAAm structure alters the signals creating diverse copolymers microstructures, depending on the molar composition between them. Besides, it has been demonstrated that none of the monomers has the tendency to give rise to blocks. At variance, an alternating tendency was found, which suggests that the reactivity monomer ratios are less than unity. However, to define more accurately the microstructure of the synthesized copolymers, and determine the actual reactivity ratio values, other experiments are currently underway and will be presented in a future work.

ACKNOWLEDGMENTS

Javier Illescas is grateful to the Consejo Nacional de Ciencia y Tecnología (CONACyT) for his postdoctoral research grant. The authors also thank the Italian Ministry of University and Scientific Research for financial support.

REFERENCES AND NOTES

1 Ionic Liquids in Synthesis, P. Wasserscheid, T. Welton, Eds.; Wiley: Weinheim, **2003**, Chapter 3, pp 41–118.

2 I. P. Vasile, C. Hardacre, *Chem. Rev.* **2007**, *107*, 2615–2665.

3 P. Kubisa, *Prog. Polym. Sci.* **2004**, *29*, 3–12.

4 U. Domansko, A. Rekawek, *J. Sol. Chem.* **2009**, *38*, 739–751.

5 C. P. Mehnert, *Chem. Eur. J.* **2005**, *11*, 50–56.

6 M. Armand, F. Endres, D. R. MacFarlane, H. Ohno, B. Scrosati, *Nat. Mater.* **2009**, *8*, 621–629.

7 M. C. Buzzeo, R. G. Evans, R. G. Compton, *Chem. Phys. Chem.* **2004**, *5*, 1106–1120.

8 Electrochemical Aspects of Ionic Liquids, H. Ohno, Ed.; Wiley Interscience: New York, **2005**, p. 408.

9 C. Roosen, P. Müller, G. Lasse, *Appl. Microbiol. Biotechnol.* **2008**, *81*, 607–614.

10 J. Dupont, J. D. Scholten, *Chem. Soc. Rev.* **2010**, *39*, 1780–1804.

11 A. Mariani, D. Nuvoli, V. Alzari, M. Pini, *Macromolecules* **2008**, *41*, 5191–5196.

12 D. Nuvoli, L. Valentini, V. Alzari, S. Scognamillo, S. Bittolo-Bon, M. Piccinini, J. Illescas, A. Mariani, *J. Mater. Chem.* **2011**, *21*, 3428–3431.

13 J. Yuan, M. Antonietti, *Polymer* **2001**, *52*, 1469–1482.

14 O. Green, S. Grubjesic, S. Lee, M. A. Firestone, *J. Macromol. Sci. Part C: Polym. Rev.* **2009**, *49*, 339–360.

15 M. D. Green, T. E. Long, *J. Macromol. Sci. Part C: Polym. Rev.* **2009**, *49*, 291–314.

16 A. Pinkert, K. N. Marsh, S. Pang, M. P. Staiger, *Chem. Rev.* **2009**, *109*, 6712–6728.

17 D. M. Haddleton, T. Welton, A. J. Carmichael, In Ionic Liquids in Synthesis, 2nd ed.; P. Wasserscheid, T. Welton, Eds.; Wiley: Weinheim, **2008**, Chapter 7, pp. 319–335.

18 J. Lu, F. Yan, J. Texter, *Prog. Polym. Sci.* **2009**, *34*, 431–448.

19 J. Salamone, S. Israel, P. Taylor, B. Snider, *Polymer* **1973**, *14*, 639–644.

20 H. Ohno, *Macromol. Symp.* **2007**, *249–250*, 551–556.

21 R. Marcilla, J. A. Blazquez, J. Rodriguez, J. A. Pomposo, D. Mecerreyes, *J. Polym. Sci. Part A: Polym. Chem.* **2004**, *42*, 208–212.

22 A. E. Visser, R. P. Swatloski, S. Griffin, D. Hartman, R. D. Rogers, *Sep. Sci. Technol.* **2001**, *36*, 785–804.

23 A. E. Visser, R. P. Swatloski, W. M. Reichert, H. James, J. Davis, R. D. Rogers, R. Mayton, S. Sheff, A. Wierzbicki, *Chem. Comm.* **2001**, *1*, 135–136.

24 T. Ueki, M. Watanabe, *Macromolecules* **2008**, *41*, 3739–3749.

25 M. Yoshizawa, H. Ohno, *Chem. Lett.* **1999**, *28*, 889–890.

26 H. Ohno, *Electrochim. Acta* **2001**, *46*, 1407–1411.

27 M. Yoshizawa, H. Ohno, *Electrochim. Acta* **2001**, *46*, 1723–1728.

28 S. Washiro, M. Yoshizawa, H. Nakajima, H. Ohno, *Polymer* **2004**, *45*, 1577–1582.

29 Z. Jiménez, C. Bounds, C. E. Hoyle, A. B. Lowe, H. Zhou, J. A. Pojman, *J. Polym. Sci. Part A: Polym. Chem.* **2007**, *45*, 3009–3021.

30 Z. Jiménez, J. A. Pojman, *J. Polym. Sci. Part A: Polym. Chem.* **2007**, *45*, 2745–2754.

31 H. Zhou, Z. Jiménez, J. A. Pojman, M. S. Paley, C. E. Hoyle, *J. Polym. Sci. Part A: Polym. Chem.* **2008**, *46*, 3766–3773.

32 J. D. Mota-Morales, M. C. Gutiérrez, M. L. Ferrer, I. C. Sanchez, E. A. Elizalde-Peña, J. A. Pojman, F. Del Monte, G. Luna-Bárcenas, *J. Polym. Sci. Part A: Polym. Chem.* **2013**, *51*, 1767–1773.

33 R. Marcilla, M. Sánchez-Paniagua, B. López-Ruiz, E. López-Cabarcos, E. Ochoteco, H. Grande, D. Mecerreyes, *J. Polym. Sci. Part A: Polym. Chem.* **2006**, *44*, 3958–3965.

34 M. Döbbelin, C. Pozo-Gonzalo, R. Marcilla, R. Blanco, J. L. Segura, J. A. Pomposo, D. Mecerreyes, *J. Polym. Sci. Part A: Polym. Chem.* **2009**, *47*, 3010–3021.

35 R. Marcilla, D. Mecerreyes, G. Winroth, S. Brovelli, M. Rodriguez, F. Cacialli, *Appl. Phys. Lett.* **2010**, *96*, 043308/1–3.

36 M. S. P. Lopez, D. Mecerreyes, E. López-Cabarcos, B. López-Ruiz, *Biosens. Bioelectron.* **2006**, *21*, 2320–2328.

37 C. Pozo-Gonzalo, R. Marcilla, M. Salsamendi, D. Mecerreyes, J. A. Pomposo, J. Rodriguez, H. J. Bolink, *J. Polym. Sci. Part A: Polym. Chem.* **2008**, *46*, 3150–3154.

38 H. Mori, Y. Ebina, R. Kambara, K. Nakabayashi, *Polym. J.* **2012**, *44*, 550–560.

39 H. Mori, M. Yahagi, T. Endo, *Macromolecules* **2009**, *42*, 8082–8092.

40 A. Brunetti, E. Princi, S. Vicini, S. Pincin, S. Bidali, A. Mariani, *Nucl. Instrum. Methods Phys. Rev. B* **2004**, *222*, 235–241.

41 K. Vijayakrishna, S. K. Jewrajka, A. Ruiz, R. Marcilla, J. A. Pomposo, D. Mecerreyes, D. Taton, Y. Gnanou, *Macromolecules* **2008**, *41*, 6299–6308.

42 M. Heskins, J. E. Guillet, *J. Macromol. Sci. Chem.* **1968**, *A2*, 1441–1455.

43 J. E. Chung, M. Yokoyama, T. Aoyagi, Y. Sakurai, T. Okano, *J. Control. Release* **1998**, *53*, 119–130.

44 A. Kumar, A. Srivastava, I. Y. Galaev, B. Mattiasson, *Prog. Polym. Sci.* **2007**, *32*, 1205–1237.

45 H. Feil, Y. H. Bae, F. J. Jan, S. W. Kim, *Macromolecules* **1993**, *26*, 2496–2500.

46 M. S. Jones, *Eur. Polym. J.* **1999**, *35*, 795–801.

47 F. Eeckman, K. Amighi, A. J. Moës, *Int. J. Pharm.* **2001**, *222*, 259–270.

48 J. Huang, X. Y. Wu, *J. Polym. Sci. Part A: Polym. Chem.* **1999**, *37*, 2667–2676.

49 H. G. Schild, D. A. Tirrell, *J. Phys. Chem.* **1990**, *94*, 4352–4356.

50 E. Kokufuta, Y. Q. Zhang, T. Tanaka, A. Mamada, *Macromolecules* **1993**, *26*, 1053–1059.

51 H. G. Schild, D. A. Tirrell, *Langmuir* **1991**, *7*, 665–671.

52 O. Wichterle, D. Lím, *Nature* **1960**, *185*, 117–118.

53 J. Kopeček, J. Yang, *Polym. Int.* **2007**, *56*, 1078–1098.

54 J. Kopeček, *Biomaterials* **2007**, *28*, 5185–5192.

55 G. Caria, V. Alzari, O. Monticelli, D. Nuvoli, J. M. Kenny, A. Mariani, S. Bidali, S. Fiori, M. Sangermano, G. Malucelli, R. Bongiovanni, A. Priola, *J. Polym. Sci. Part A: Polym. Chem.* **2009**, *47*, 1422–1428.

56 S. Scognamillo, V. Alzari, D. Nuvoli, A. Mariani, *J. Polym. Sci. Part A: Polym. Chem.* **2010**, *48*, 2486–2490.

57 S. Scognamillo, V. Alzari, D. Nuvoli, A. Mariani, *J. Polym. Sci. Part A: Polym. Chem.* **2010**, *48*, 4721–4725.

58 S. Scognamillo, C. Bounds, M. Luger, A. Mariani, J. A. Pojman, *J. Polym. Sci. Part A: Polym. Chem.* **2010**, *48*, 2000–2005.

59 S. Russo, A. Mariani, V. N. Ignatov, I. I. Ponomarev, *Macromolecules* **1993**, *26*, 4984–4985.

60 S. Scognamillo, V. Alzari, D. Nuvoli, J. Illescas, S. Marceddu, A. Mariani, *J. Polym. Sci. Part A: Polym. Chem.* **2011**, *49*, 1228–1234.

61 V. Alzari, A. Mariani, O. Monticelli, L. Valentini, D. Nuvoli, M. Piccinini, S. Scognamillo, S. Bittolo Bon, J. Illescas, *J. Polym. Sci. Part A: Polym. Chem.* **2010**, *48*, 5375–5538.

62 R. Sanna, V. Alzari, D. Nuvoli, S. Scognamillo, S. Marceddu, A. Mariani, *J. Polym. Sci. Part A: Polym. Chem.* **2012**, *50*, 1515–1520.

63 R. Sanna, D. Sanna, V. Alzari, D. Nuvoli, S. Scognamillo, M. Piccinini, M. Lazzari, E. Gioffredi, G. Malucelli, A. Mariani, *J. Polym. Sci. Part A: Polym. Chem.* **2012**, *50*, 4110–4118.

64 R. Sanna, E. Fortunati, V. Alzari, D. Nuvoli, A. Terenzi, M. F. Casula, J. M. Kenny, A. Mariani, *Cellulose* **2013**, *20*, 2393–2402.

65 V. Alzari, D. Nuvoli, R. Sanna, L. Peponi, M. Piccinini, S. Bittolo Bon, S. Marceddu, L. Valentini, J. M. Kenny, A. Mariani, *Colloid Polym. Sci.* **2013**, *291*, 2681–2687.

66 J. W. Seo, J. Y. Hwangab, U. S. Shin, *RSC Adv.* **2014**, *4*, 26738–26747.

67 R. S. Varma, V. V. Namboodiri, *Pure Appl. Chem.* **2001**, *73*, 1309–1313.

68 J. F. Lutz, K. Weichenhan, O. Akdemir, *A. Hoth Macromolecules* **2007**, *40*, 2503–2508.

69 T. Kawaguchi, Y. Kojima, M. Osa, T. Yoshizaki, *Polym. J.* **2008**, *40*, 455–459.

70 L. C. Dong, A. S. Hoffman, *J. Control. Rel.* **1991**, *15*, 141–152.

71 S. Furyk, Y. J. Zhang, D. Ortiz-Acosta, P. S. Cremer, D. E. Bergbreiter, *J. Polym. Sci. Part A: Polym. Chem.* **2006**, *44*, 1492–1501.

72 C. M. Schilli, M. F. Zhang, E. Rizzardo, S. H. Thang, Y. K. Chong, K. Edwards, G. Karlsson, A. H. E. Müller, *Macromolecules* **2004**, *37*, 7861–7866.

73 K. Tauer, M. Mukhamedjanova, C. Holtze, P. Nazaran, J. Lee, *Macromol. Symp.* **2007**, *248*, 227–238.

74 N. Singh, L. A. Lyon, *Colloid Polym. Sci.* **2008**, *286*, 1061–1069.

75 C. W. Liew, Y. S. Ong, J. Y. Lim, C. S. Lim, K. H. Teoh, S. Ramesh, *Int. J. Electrochem. Sci.* **2013**, *8*, 7779–7794.

76 Infra-Red Spectra and Structure of Organic Long-Chain Polymers; A. Elliot, Ed.; St. Martin's Press: New York, **1969**, p. 32.

77 M. Takafuji, S. Ide, T. Ihara, Z. Xu, *Chem. Mater.* **2004**, *16*, 1977–1983.

78 M. Liu, F. Bian, F. Sheng, *Eur. Polym. J.* **2005**, *41*, 283–291.

79 V. Alzari, O. Monticelli, D. Nuvoli, J. M. Kenny, A. Mariani, *Biomacromolecules* **2009**, *10*, 2672–2677.

80 F. Zeng, Z. Tong, H. Feng, *Polymer* **1997**, *38*, 5539–5544.

81 T. Hirano, T. Anmoto, N. Umezawa, H. Momose, Y. Katsumoto, M. Oshimura, K. Ute, *Polym. J.* **2012**, *44*, 815–820.

82 N. Pekel, Z. M. O. Rzaev, O. Güven, *Macromol. Chem. Phys.* **2004**, *205*, 1088–1095.

83 C. Damas, S. Baggio, A. Brembilla, P. Lochon, *Eur. Polym. J.* **1997**, *33*, 1219–1224.

84 V. Alzari, D. Nuvoli, S. Scognamillo, M. Piccinini, E. Gioffredi, G. Malucelli, S. Marceddu, M. Sechi, V. Sanna, A. Mariani, *J. Mater. Chem.* **2011**, *21*, 8727–8733.

85 V. Alzari, D. Nuvoli, R. Sanna, S. Scognamillo, M. Piccinini, J. M. Kenny, G. Malucelli, A. Mariani, *J. Mater. Chem.* **2011**, *21*, 16544–16549.